

Annual Project Summary

Fault Loading Processes in the New Madrid Seismic Zone (collaborative work with Stanford University)

Award Number 02HQGR0120

Shelley J. Kenner

Department of Geological Sciences, University of Kentucky

Phone: (859) 257-5506; Fax: (859) 323-1938; Email: skenner@uky.edu

NEHRP Elements: II. Develop theoretical models of fault loading in low strain-rate environments

Keywords: Seismotectonics

1 Introduction

Our understanding of the tectonic processes which generate intraplate earthquakes such as in the New Madrid seismic zone is severely limited. There are, as yet, no widely agreed upon mechanical models for such earthquakes. We are developing tectonically reasonable finite element models (FEM) for the generation of intraplate earthquake sequences, including the effects of glacial unloading on seismicity. During the present reporting period we focused on testing and refining FEM methods for computing stresses induced by glacial advance and recession. Secondly, we worked to implement methods that will allow for the rheological refinement of models initially developed by Kenner and Segall [1] and the synthesis of local faulting models with regional glacial rebound models.

2 Finite element implementation and benchmarking of viscoelastodynamics

This section describes the implementation of the equations governing the loading of a viscoelastic Earth in a finite element context and also presents the results of benchmark tests.

2.1 Governing equations

Due to the presence of an initial stress field in the Earth, the equations governing stress and displacement in a viscoelastic, layered medium in response to a surface load are usually expressed as perturbations from a pre-existing equilibrium state. The necessary equations are the incremental momentum balance, the incremental continuity equation and the incremental constitutive equation. Most finite element packages correctly handle the continuity and constitutive equations and we will therefore not consider these here.

The material incremental momentum equation for quasi-static, infinitesimal perturbations of a stratified, compressible, fluid Earth initially in hydrostatic equilibrium subject to gravitational forces but neglecting inertial forces is [2, 3]

$$\sigma_{ij,j}^{\delta} + (p_{,j}^0 u_j)_{,i} + \rho^{\Delta} g_i^0 + \rho^0 g_i^{\Delta} = 0 \quad (1)$$

where σ is the Cauchy stress tensor defined as positive in tension, $p = -\sigma_{kk}/3$ is the pressure, ρ the density, g the gravitational acceleration and u the displacement. The superscripts 0, δ and Δ denote the initial, material

incremental and local incremental fields respectively. The usual summation and differentiation conventions apply to the index notation. The first term in Eq. 1 describes the force from spatial gradients in stress. The second term concerns the incremental stress resulting from a particle's displacement in the initial stress field, parallel to the stress gradient. This term is commonly referred to as "pre-stress advection". The third and fourth term describe perturbations to the gravitational forces due to changes in density and gravitational acceleration, respectively. The third term is sometimes referred to as the buoyancy term, which, together with the second term, accounts for isostasy.

The momentum equation is frequently simplified by ignoring the change in the gravitational field within, that is neglecting the fourth term which is insignificant except at the very longest wavelengths. A model with this approximation is described as non-self-gravitating. Further simplification is obtained for a layer that is uniform in density and incompressible, since the third term in Eq. 1 vanishes. For a non-self-gravitating incompressible uniform Earth the momentum equation can be rewritten in terms of the local incremental stress as

$$\sigma_{ij,j}^{\Delta} = 0 \quad (2)$$

$$\sigma_{ij}^{\Delta} = \sigma_{ij}^{\delta} + p_{,k}^0 u_k \delta_{ij} = \sigma_{ij}^{\delta} + \rho^0 g^0 u_k \delta_{ij} \quad (3)$$

We will use this simplified equation for the finite element modeling.

2.2 Implementation of the viscoelastodynamic equations into Finite Element codes

We are indebted to Prof. P. Wu for invaluable help on the implementation of the simplified viscoelastodynamic momentum equation into Abaqus, our commercial finite element analysis package. The following paragraphs are based on discussions with, and a manuscript by, Prof. Wu.

Most commercial finite element packages are mainly designed for engineering applications where only the divergence of the stress tensor is included in the momentum equation, $S_{ij,j} = 0$, ignoring isostasy and self-gravitation. This makes the modeling codes unsuitable for geophysical applications involving long wavelengths and non-elastic deformation [4]. If we, however, consider our model as non-self-gravitating and the elements as incompressible and uniform in density, we can utilize Eqs. 2 and 3 to define a new, finite element stress tensor as

$$\mathbf{S}^{\text{FE}} = \mathbf{S} - \rho^0 g^0 u_z \mathbf{I} \quad (4)$$

where u_z is the displacement in the vertical direction, parallel to the gravity field, and \mathbf{I} is the identity matrix. Differentiation gives us

$$S_{ij,j}^{\text{FE}} = S_{ij,j} - \rho^0 g^0 u_{z,j} \delta_{ij} = 0 \quad (5)$$

which is the momentum equation we desire, expressed in terms of the new stress. Due to the transformation in Eq. 4, new boundary conditions must be applied to the finite elements. In the following, P is the surface load, the index h signifies a horizontal coordinate and $[F]_{Z-}^{Z+} = \lim_{\epsilon \rightarrow 0} (F(Z + \epsilon) - F(Z - \epsilon))$.

1. At the Earth's surface: $S_{zz}^{\text{FE}} + \rho^0 g^0 u_z|_{z=0} = P$, assuming the density of air to be zero, and $S_{hz}^{\text{FE}}|_{z=0} = 0$
2. At solid-solid interfaces at depth Z : $[S_{zz}^{\text{FE}}]_{Z-}^{Z+} = (\rho_+ - \rho_-)g^0 u_z$ and $[S_{hz}^{\text{FE}}]_{Z-}^{Z+} = [u_h]_{Z-}^{Z+} = [u_z]_{Z-}^{Z+} = 0$

These boundary conditions are easily implemented in finite element packages as Winkler, or elastic, foundations with spring constants $\rho^0 g^0$ or $(\rho_+ - \rho_-)g^0$, respectively. All non-vertical material interfaces should have these foundations attached.

Finally, due to the transformation in Eq. 4, the stress output after a finite element model run has to be converted back to the "correct" stress through $\mathbf{S} = \mathbf{S}^{\text{FE}} + \rho^0 g^0 u_z \mathbf{I}$. This conversion is crucial since stress magnitudes otherwise will be much too low. Displacements in the finite element model are not affected by the transformation and, therefore, need no postprocessing.

2.3 Benchmark tests of the Finite Element implementation

We implemented the Winkler foundation formalism discussed above in our finite element package Abaqus and performed a number of benchmark tests. Three of these tests will be discussed below. Our models below all have an interior area of good resolution approximately 2500x2000 km, increasing element size away from the interior out to 10000x5000 km and infinite elements to the sides and at the bottom. The models have not been optimized for efficiency or accuracy, we have simply used models that seem “big enough”.

2.3.1 Viscoelastic half-space in 2D with a boxcar Heaviside load

The solution for the response of a viscoelastic half-space to an impulsive boxcar load with uniform amplitude is well known, e.g. [5]. The vertical displacement at the surface is given in the wave-number domain by

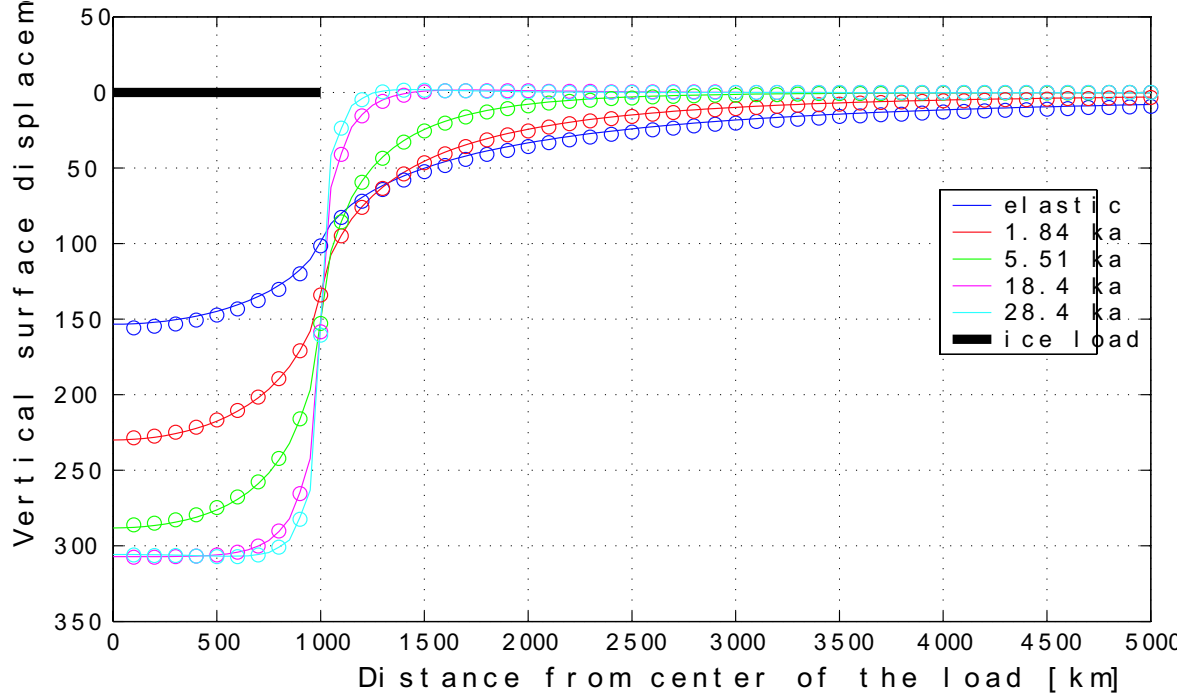


Figure 1: Vertical surface displacement of a viscoelastic half-space subject to a Heaviside load. Lines are finite element modeling results and circles are results from the transform method. Times are in 1000 years after the application of the load.

$$\int_{-\infty}^{\infty} \frac{-PL(k)}{\rho g + 2\mu k} \left[1 + \frac{2\mu k}{\rho g} (1 - e^{-\alpha}) \right] e^{ikx} dk \quad (6)$$

where P is the amplitude of the boxcar load and $L(k)$ its wave-number k domain representation. α is the relaxation time given by

$$\alpha = \frac{\rho g \mu}{\eta(\rho g + 2\mu k)} \quad (7)$$

We evaluated Eq. 6 numerically using a Fast Fourier Transform (FFT) and compared our finite element calculations to the FFT result. Figure 1 shows the comparison of the two methods for a 15 MPa 2D boxcar load with 1000 km half-length applied to a 2D, incompressible, non-self-gravitating viscoelastic half-space with the following parameters:

Density	5000 kg/m ³
Young's modulus	113 GPa
Viscosity	1.45×10^{21} Pa s
Poisson's ratio	0.5
Gravity	9.82 m/s ²

As Figure 1 shows, the two methods agree extremely well for the vertical surface displacements. Our results also agree well with the finite element calculations of [6], for a similar 2D model, both in terms of vertical surface displacements and Mises stress.

2.3.2 Axisymmetric viscoelastic half-space with a boxcar Heaviside load

We compared our finite element model of an axisymmetric viscoelastic half-space subject to an impulsive boxcar load with the finite element model of [7]. The results for vertical surface displacements agree very well, although the comparison in this case was visual rather than numerical.

2.3.3 Elastic plate overlying a viscoelastic half-space

We tested our finite element implementation against the transform method results of [8]. The tested model is an axisymmetric model with an elastic plate overlying a viscoelastic half-space. The model is subjected to an ice load of elliptic cross-section, 2.8 km high at the center with a density of 0.91 kg/m³. The loading history is a simplified representation of the final Weichselian glaciation in Fennoscandia, the load is linearly increased over 90 kyr to its maximum, referred to as the Last Glacial Maximum (LGM), and then linearly decreased to zero over 10 kyr, End of Glaciation (EoG). The model is run for an additional 8 kyr up to current times. Parameters of the model are:

Layer	1	Half-space
Density	3380	3380 kg/m ³
Young's modulus	192	435 GPa
Viscosity	∞	1.0×10^{21} Pa s
Poisson's ratio	0.5	0.5
Gravity	9.81	9.81 m/s ²

Figure 2 shows the result of our modeling and comparing to similar figures in [8], the results are remarkably similar. Maximum shear stress contours agree both in shape and numerically and the stress states are very similar, although not identical. This could be due to the algorithm used to evaluate the state of stress, and also to the relative isotropy of the stress state in parts of the model.

3 Development of more realistic models of earthquake generation due to transient relaxation of a localized weak zone

3.1 Refinement of the numerical implementation of fault failure criteria

One of the goals of this proposal is a further exploration of the parameter space associated with earthquake generation via a relaxing zone of relative weakness in the lower crust. The original models of Kenner and Segall [1] invoke a fault failure criteria that evaluates stresses at each node independently. As a result, each model took 6-10 days to run. To facilitate a more expedient exploration of the parameter space, the numerical implementation of the fault failure criteria has been rewritten to reduce time spent on data I/O. Furthermore, versions of the code now exist which allow for fault failure criteria based on averaged stresses at a predefined set of nodes. When warranted, implementation of nodal averaging will also reduce processing time. As greater complexity is added to the model, in the form of time-dependent boundary conditions from glacial rebound models, reductions in processing time will become particularly important.

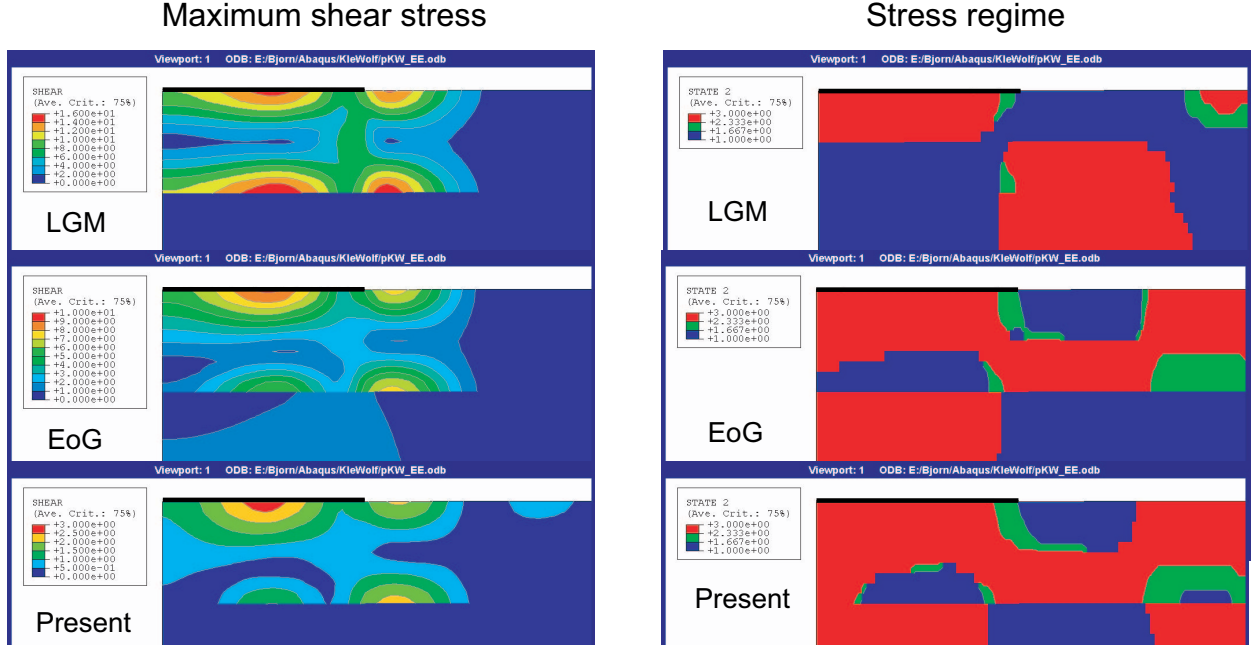


Figure 2: Maximum shear stress contours and state of stress in the model at three different times. At LGM the full load is on the model, 10 kyr later at EoG the load has disappeared and Present is additionally 8 kyr later. The extent of the ice load is indicated by a black bar on top of the plots.

3.2 Implementation of alternative viscoelastic rheologies

The models of Kenner and Segall [1] included a Maxwell viscoelastic weak zone embedded within an elastic body. For zero applied strain-rate, stresses in a Maxwell viscoelastic body relax to zero. It is more likely that weak zones in intraplate regions maintain some long-term elastic strength. This can be modeled using a variety of other linear viscoelastic materials including Voight or standard linear solid rheologies.

Methods have now been developed which will allow for the incorporation of arbitrary linear viscoelastic rheologies in finite element models of earthquake generation using a Prony series description of the constitutive law. In this formulation, the time-dependent dilatational relaxation modulus, $G(\tau)$, has the form

$$G(\tau) = G_{\infty} + \sum_{i=1}^{n_G} G_i e^{-\frac{\tau}{\tau_i}} \quad (8)$$

where G_{∞} is the long-term shear modulus and τ_i are relaxation times associated with moduli G_i . This approach is also computationally faster than our previous method for incorporating Maxwell viscoelastic rheologies.

References

- [1] Kenner, S.J. and P. Segall, A mechanical model for intraplate earthquakes: Application to the New Madrid Seismic Zone. *Science*, **289**, 2329-2332, 2000.
- [2] Wolf, D., Viscoelastodynamics of a stratified, compressible planet: incremental field equations and short- and long-time asymptotes. *Geophys. J. Int.*, **104**, 401–417, 1991.
- [3] Johnston, P., P. Wu and K. Lambeck, Dependence of horizontal stress magnitude on load dimension in glacial rebound models. *Geophys. J. Int.*, **132**, 41–60, 1998.

- [4] Wu, P., Viscoelastic versus viscous deformation and the advection of pre-stress. *Geophys. J. Int.*, **108**, 136–142, 1992.
- [5] Wolf, D., On Boussinesq's problem for Maxwell continua subject to an external gravity field. *Geophys. J. R. astr. Soc.*, **80**, 275–279, 1985.
- [6] Wu, P., Deformation of an incompressible viscoelastic flat earth with power-law creep: a finite element approach. *Geophys. J. Int.*, **108**, 35–51, 1992.
- [7] Wu, P., Postglacial rebound in a power-law medium with axial symmetry and the existence of the transition zone in relative sea-level data. *Geophys. J. Int.*, **114**, 417–432, 1993.
- [8] Klemann, V. and D. Wolf, Modelling of stresses in the Fennoscandian lithosphere induced by Pleistocene glaciations. *Tectonophysics*, **294**, 291–303, 1998.